



**NIST National Standard Reference Data Series
NIST NSRDS 64-2023**

**NIST Electron Elastic-Scattering
Cross-Section Database**

*Version 5.0
User's Guide*

A. Jablonski
F. Salvat
C. J. Powell

This publication is available free of charge from:
<https://doi.org/10.6028/NIST.NSRDS.64-2023>

NIST National Standard Reference Data Series
NIST NSRDS 64-2023

NIST Electron Elastic-Scattering
Cross-Section Database

Version 5.0
User's Guide

A. Jablonski
Polish Academy of Sciences

F. Salvat
Universitat de Barcelona, Barcelona

C. J. Powell
Materials Measurement Science Division
Material Measurement Laboratory
National Institute of Standards and Technology

This publication is available free of charge from:
<https://doi.org/10.6028/NIST.NSRDS.64-2023>

December 2023



U.S. Department of Commerce
Gina M. Raimondo, Secretary

National Institute of Standards and Technology
Laurie E. Locascio, NIST Director and Under Secretary of Commerce for Standards and Technology

The National Institute of Standards and Technology (NIST) uses its best efforts to deliver a high quality version of the database and to verify that the data contained therein have been selected on the basis of sound scientific judgment. However, NIST makes no warranties to that effect, and NIST shall not be liable for any damage that may result from errors or omissions in the database.

Certain trade names and company products are mentioned in the text to specify adequately the computer products and equipment needed to use this software. In no case does such identification imply endorsement by the National Institute of Standards and Technology of these computer products and equipment, nor does it imply that the products are necessarily the best available for the purpose.

Publication History

Approved by the NIST Editorial Review Board on 2023-11-28

Supersedes NIST NSRDS 64 (September 2016) <http://dx.doi.org/10.6028/NIST.NSRDS.64>

For a literature citation, the database should be viewed as a book published by NIST. The citation would therefore be:

A. Jablonski, F. Salvat, C. J. Powell, and A. Y. Lee, *NIST Electron Elastic-Scattering Cross-Section Database - Version 5.0*, National Institute of Standards and Technology, Gaithersburg, MD (2023);
<https://srdata.nist.gov/srd64/>, retrieved [date of access].

How to Cite this NIST Technical Series Publication

Jablonski A, Salvat F, Powell CJ (2023) NIST Electron Elastic-Scattering Cross-Section Database, Version 5.0, User's Guide. (National Institute of Standards and Technology, Gaithersburg, MD), NIST National Standard Reference Data Series (NSRDS) NIST NSRDS 64-2023. <https://doi.org/10.6028/NIST.NSRDS.64-2023>

NIST Author ORCID ID

C. J. Powell 0000-0001-8990-2286

©2023 copyright by the U.S. Secretary of Commerce on behalf of the United States of America. All rights reserved. No part of this database may be reproduced, stored in a retrieval system, or transmitted, in any form or by any means, electronic, mechanical, photocopying, recording, or otherwise, without the prior written permission of the distributor.

TABLE OF CONTENTS

1. Introduction	1
2. Operation of the Database	4
2.1 Elastic-Scattering Cross Sections	4
2.2 Transport Cross Sections	10
2.3 Sampler of Elastic Scattering Angles	14
2.4 Search	15
2.5 More Options	15
3. Theory	15
3.1 Differential Cross Sections for Elastic Scattering	15
3.2 Transport Cross Sections	19
4. References	20
APPENDIX A Sampler of Elastic Scattering Angles	21
APPENDIX B Contacts	27

1. Introduction

Theoretical description of electron transport in solids is important in radiation physics, electron lithography, electron-probe microanalysis, analytical electron microscopy, and surface analysis by Auger electron spectroscopy (AES) and X-ray photoelectron spectroscopy (XPS). In these and other applications, the trajectories of electrons in a solid are generally modified by single and multiple elastic-scattering events. An evaluation of the effects of elastic scattering on the process of interest requires knowledge of the cross sections for electron elastic scattering by the constituent atoms of the particular solid. Although calculated and measured electron elastic-scattering cross sections are available in the literature for selected elements and a limited number of electron energies, this information is incomplete and insufficient for general use.

NIST released Version 1.0 of the Elastic-Electron-Scattering Cross-Section Database (SRD 64) in 1996. This version provided differential and total elastic-scattering cross sections for elements with atomic numbers from 1 to 96 and for electron energies between 50 eV and 9999 eV in steps of 1 eV. These cross sections were calculated using the Thomas-Fermi-Dirac potential to describe the interaction between an electron and an atom, and using both relativistic and non-relativistic models. This version was designed for analyses of the transport of signal electrons in AES and XPS although it could, of course, be used for other applications.

Version 2.0 of the database was released in 2000. In this version, the upper electron-energy limit was extended to 20 keV, and phase shifts and transport cross sections were also provided. The elastic-scattering cross sections, phase shifts, and transport cross sections, however, were obtained only with a relativistic model because this was believed to be more reliable than the non-relativistic model.

Version 3.0 of the database was released in 2002, and contained two major changes. First, the differential elastic-scattering cross sections, total elastic-scattering cross sections, phase shifts, and transport cross sections were calculated from a relativistic Dirac partial-wave analysis in which the potentials were obtained from Dirac-Hartree-Fock electron densities computed self-consistently for free atoms. This potential is believed to be more reliable than the Thomas-Fermi-Dirac potential used previously [1]. Differences in elastic-scattering cross sections and transport cross sections resulting from this change of potential were described in a review article [1].

In addition, it is possible in Version 3.0 to create and/or print files illustrating variation of differential elastic-scattering cross sections versus scattering angle for one or more elements or for one or more energies. Some of the database screens were redesigned as a result of the increase in the upper electron-energy limit to 300 keV.

Version 3.1 of the database, issued in August, 2003, contains two corrections to Version 3.0. First, a numerical mistake was found in the calculation of differential cross sections for a small number of elements and energies (e.g., F at 300 eV). Second, the routine used for interpolations between differential cross sections at certain scattering angles was found to be inadequate in the vicinity of deep minima in the differential cross sections (e.g., Cu at 319 eV). The libraries of cross-section data and the software have been revised to correct these problems.

Version 3.2 of the database was issued in December, 2010. The installation program for Version 3.2 was changed so that it would operate on newer versions of the Windows operating system. There were no changes or additions to the data in the database although a new About box was added to the main menu. This box shows two references, a 2004 critical review [1] and a 2005 review [2], that discuss evaluations of the compiled data, methods of determination, and uncertainty.

Version 3.2 of the Electron Elastic-Scattering Cross-Section Database had the following capabilities:

- Graphical display of differential elastic-scattering cross sections in different coordinate systems
- Graphical display of the dependence of transport cross sections on electron energy
- Display of numerical values of differential elastic-scattering cross sections, total elastic-scattering cross sections, and transport cross sections
- Creation of files containing differential elastic-scattering cross sections for specified elements, energies and coordinates
- Creation of files containing plots of differential elastic-scattering cross sections versus scattering angle for one or more elements or for one or more electron energies
- Creation of files containing phase shifts for specified elements and for energies up to 20,000 eV
- Creation of files containing transport cross sections for specified elements and energies
- Creation of random number generators providing the polar scattering angles to be used in Monte Carlo simulations of electron transport in solids; and
- Runs of the random number generators

Version 4.0 of the database was released in August, 2016. The database has been redesigned to operate in a user's browser rather than as an installed database on a personal computer with the Windows operating system. All screens have been redesigned. The database now provides differential elastic-scattering cross section and transport cross sections, as in previous versions. Graphical displays of these cross sections are available as before. Three types of data files can be downloaded:

- Javascript object notation (JSON) files
- Comma separated variable (CSV) files that can be opened by spreadsheet software
- Text files that can be easily read by user programs.

Phase Shifts are not provided in Version 4.0 of the database.

Version 5.0 of the database was released in December 2023. Most screens were redesigned. An option was added to provide samplers of polar elastic-scattering angles that can be used in Monte Carlo simulations of electron transport in solids (as was possible in Version 3.2 and earlier versions). However, a more accurate numerical method has been implemented in Version 5.0, as described in Appendix A. The new sampler is designed to generate scattering angles for electron energies between 50 eV and 20 keV.

The differential elastic-scattering cross sections (DCSs) were calculated using the relativistic Dirac partial-wave method, as described by Walker [3]. The scattering potential was obtained from the self-consistent Dirac-Hartree-Fock electron density for free atoms [4] with the local exchange potential of Furness and McCarthy [5]. The numerical calculations were performed with the algorithm described by Salvat and Mayol [6]. Transport cross sections were calculated from the DCSs as described by Jablonski et al. [1].

Cross sections are expressed in units of the square of the Bohr radius, a_0 , which is $0.52917721 \times 10^{-10}$ m.

2. Operation of the Database

Version 5.0 of the database has been designed to make operation of the database as easy and intuitive as possible. Help information is available on many of the screens.

Figure 1 shows the upper portion of the introductory screen. A user can click on one of the first two main menu options in the left part of this screen, **Elastic-Scattering Cross Sections** or **Transport Cross Sections**, to go directly to screens that will provide the desired data after selection of an element from the Periodic Table, as described in Sections 2.1 or 2.2, respectively. Alternatively, a user can choose to click on the third main menu option, **Sampler of Elastic Scattering Angles**, to obtain samplers of polar elastic-scattering angles that can be used in Monte Carlo simulations of electron transport in solids, as described in the Appendix. The **More Options** choice will be described in Section 2.3.

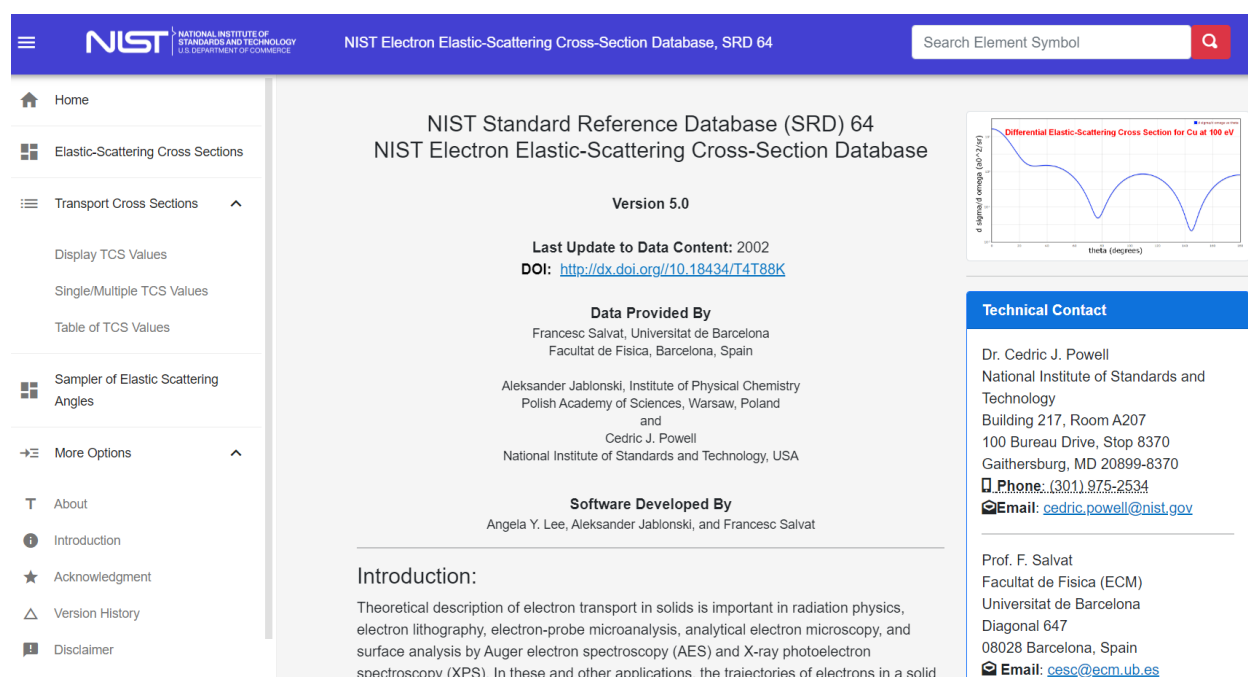


Fig. 1. Upper portion of the introductory screen.

2.1 Elastic-Scattering Cross Sections

After clicking on **Elastic-Scattering Cross Sections**, the first main menu option on the introductory screen, a Periodic Table of the elements will appear, as shown in Fig. 2. The user will then click on the symbol of the desired element and the screen of Fig. 3 will appear. For the example screen of Fig. 3, Au has been chosen together with an electron energy of 50 eV.

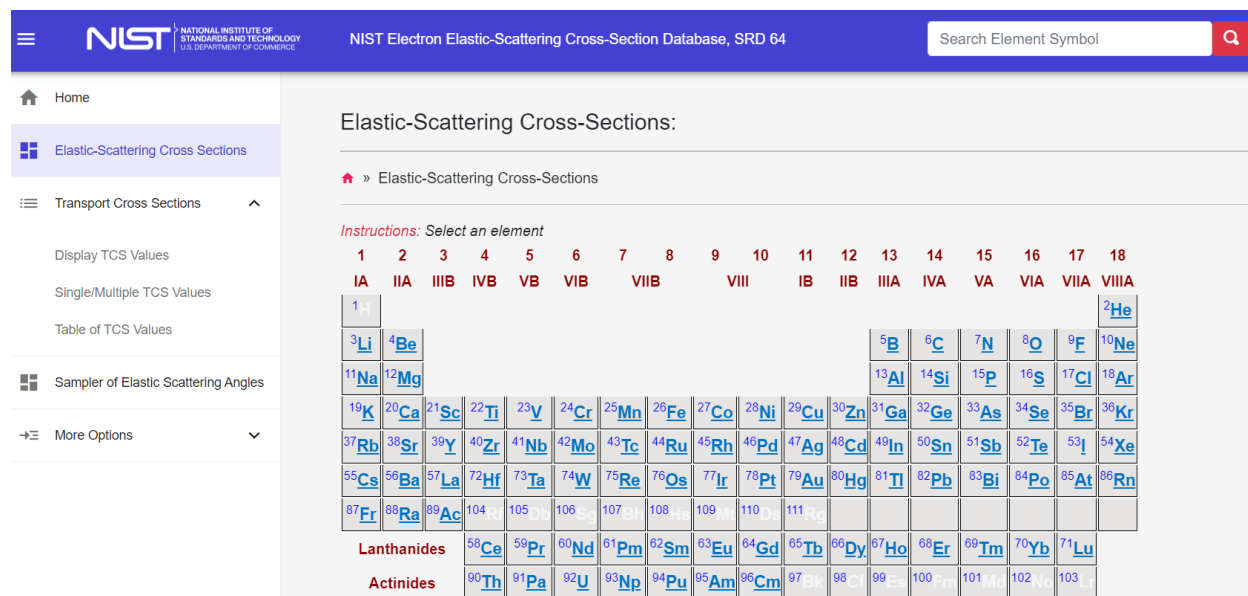


Fig. 2. Screen for selecting an element.

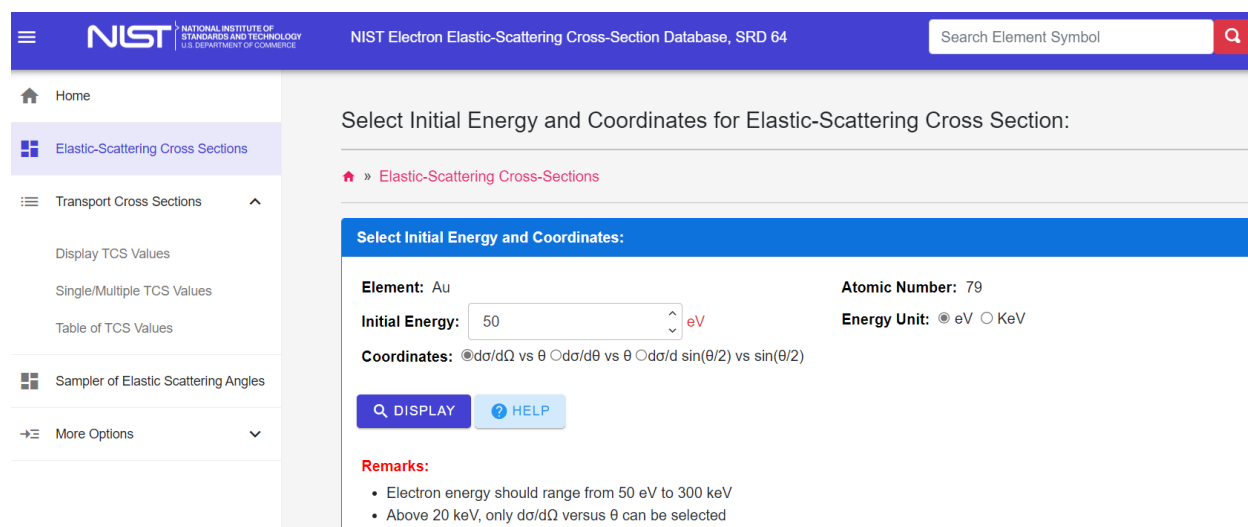


Fig. 3. Screen for selecting electron energy and coordinates.

A selection then needs to be made in the screen of Fig. 3 of the coordinates for display of the differential elastic-scattering cross section. Three coordinate systems are available for electron energies of 20 keV and below in which the differential elastic-scattering cross section is expressed with respect to solid angle Ω , polar scattering angle θ , or $\sin(\theta/2)$:

- (a) $d\sigma/d\Omega$ versus θ
- (b) $d\sigma/d\theta$ versus θ
- (c) $d\sigma/d\sin(\theta/2)$ versus $\sin(\theta/2)$

In the latter case, the cross section $d\sigma/d\sin(\theta/2)$ is related to the differential cross section for electron momentum change $d\sigma/dq$. The quantity q is defined by $q = |\mathbf{K}' - \mathbf{K}|$ where \mathbf{K} and \mathbf{K}' are wave vectors before and after an elastic collision. We have:

$$\frac{d\sigma}{d\sin(\theta/2)} = 2K \frac{d\sigma}{dq}$$

where $K = |\mathbf{K}|$. For electron energies of 20 001 eV and above, cross sections are available only in $d\sigma/d\Omega$ versus θ coordinates.

The elastic-scattering cross sections calculated by the database are expressed in units involving the square of the Bohr radius a_0 (the radius of the first Bohr orbit of the hydrogen atom) where $a_0 = 5.291\,772\,1 \times 10^{-11}$ m and $a_0^2 = 2.800\,285\,2 \times 10^{-21}$ m². The specific units for the cross sections in the different coordinate systems are as follows:

- (a) a_0^2 /steradian for the $d\sigma/d\Omega$ versus θ coordinate system;
- (b) a_0^2 /radian for the $d\sigma/d\theta$ versus θ coordinate system; and
- (c) a_0^2 for the $d\sigma/d\sin(\theta/2)$ versus $\sin(\theta/2)$ coordinate system.

These units are used in the screen displays and in the files created by the database.

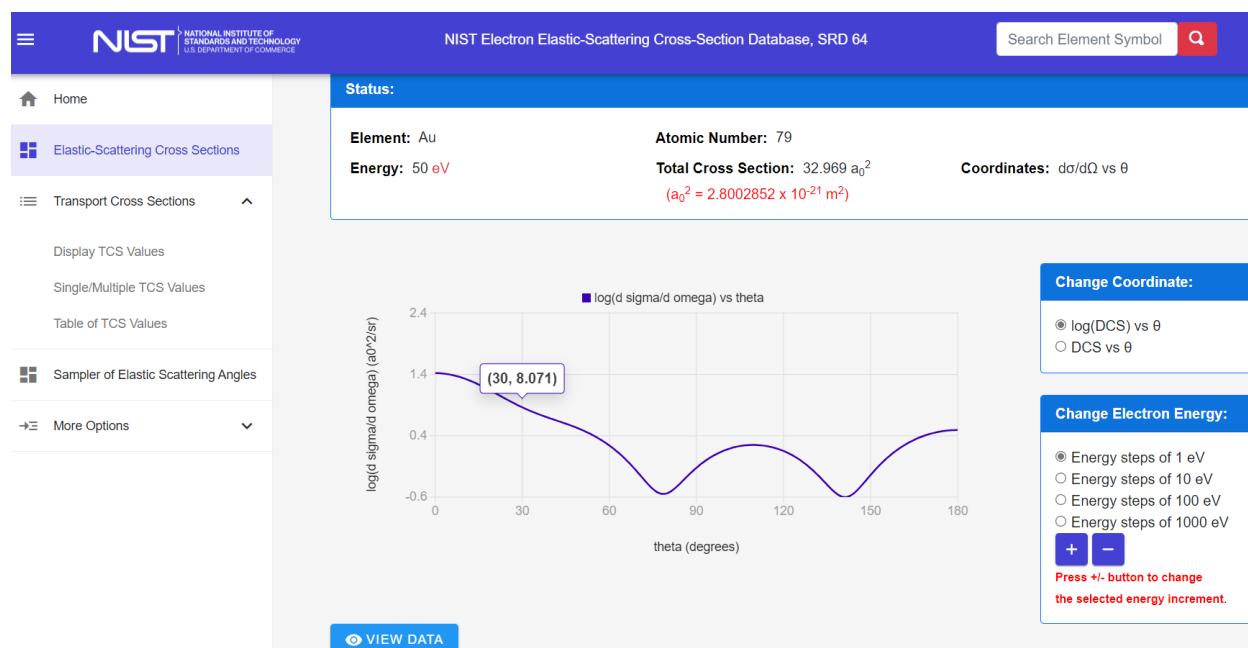


Fig. 4(a). Screen showing the differential cross section for Au in $d\sigma/d\Omega$ versus θ coordinates at 50 eV on semi-logarithmic scales.

After selection of the electron energy and the coordinate system on the screen of Fig. 3, the user will click **Display** and the screen of Fig. 4(a) will appear. For this example, the DCS for Au in the $d\sigma/d\Omega$ versus θ coordinate system is shown for an energy of 50 eV.

For cross sections in $d\sigma/d\Omega$ versus θ coordinates and for electron energies of 20 keV and below, the differential cross sections can be displayed on logarithmic or linear scales versus polar scattering angle on a linear scale. For Fig. 4(a), the DCS is displayed on a semi-logarithmic scale

while the DCS on a linear scale is shown in Fig. 4(b). If the cursor is placed near the plotted curve, values of the DCS will be given for a particular value of θ , as shown in Figs. 4(a) and 4(b).

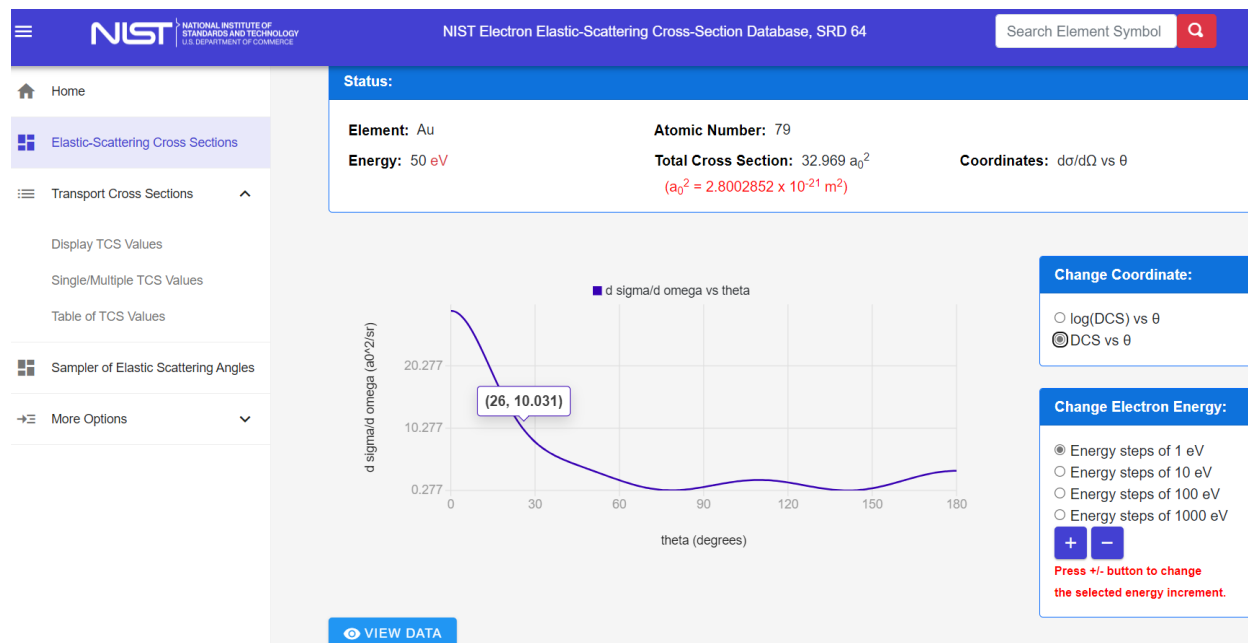


Fig. 4(b). Screen showing the differential cross section for Au in $d\sigma/d\Omega$ versus θ coordinates at 50 eV on linear scales.

The initially selected energy can be changed by clicking the + **energy** or - **energy** buttons; these changes will occur in steps of 1 eV, 10 eV, 100 eV, or 1000 eV (within the range 50 eV to 20 keV). The total cross section for the selected energy is given above the plot.

For electron energies of 20 001 eV and above, the differential cross sections can be displayed only in $d\sigma/d\Omega$ versus θ coordinates. Displays can be shown on logarithmic scales, as shown in Fig. 5(a), or on semi-logarithmic scales, as shown in Fig. 5(b). For these examples, the DCS for Au is shown for an energy of 50 keV. The initially selected energy can be varied in steps of 10 eV, 100 eV, 1 keV, or 10 keV.

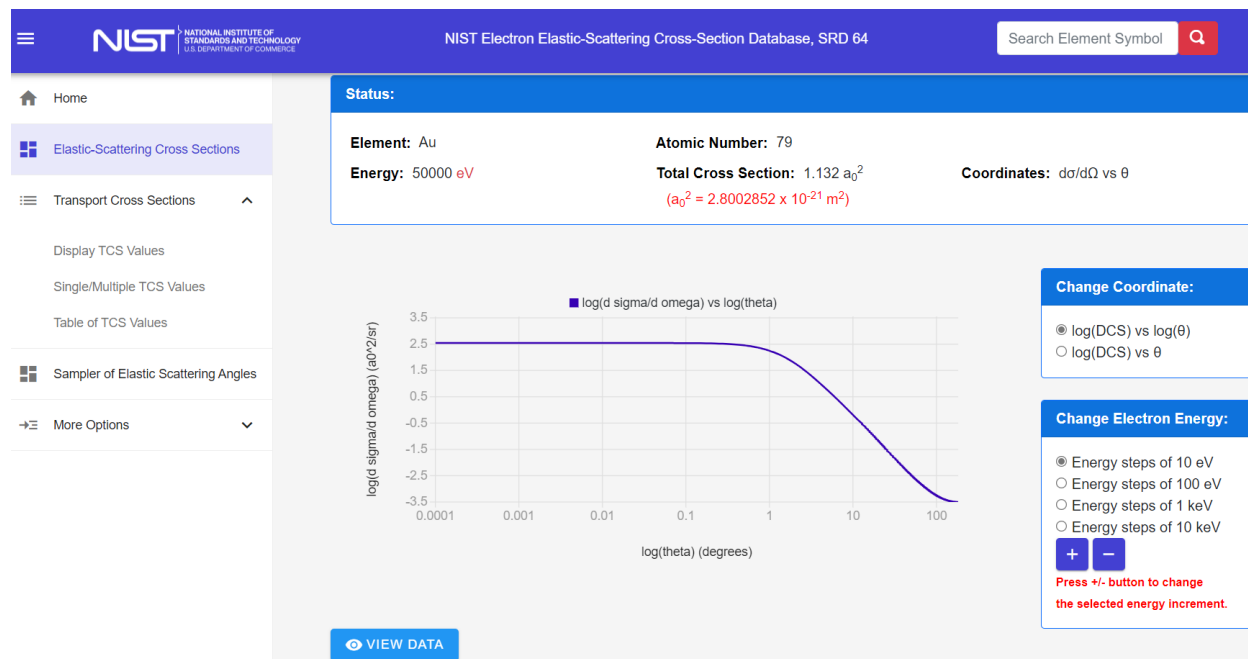


Fig. 5(a). Screen showing the differential cross section for Au in $d\sigma/d\Omega$ versus θ coordinates at 50 keV on logarithmic scales.

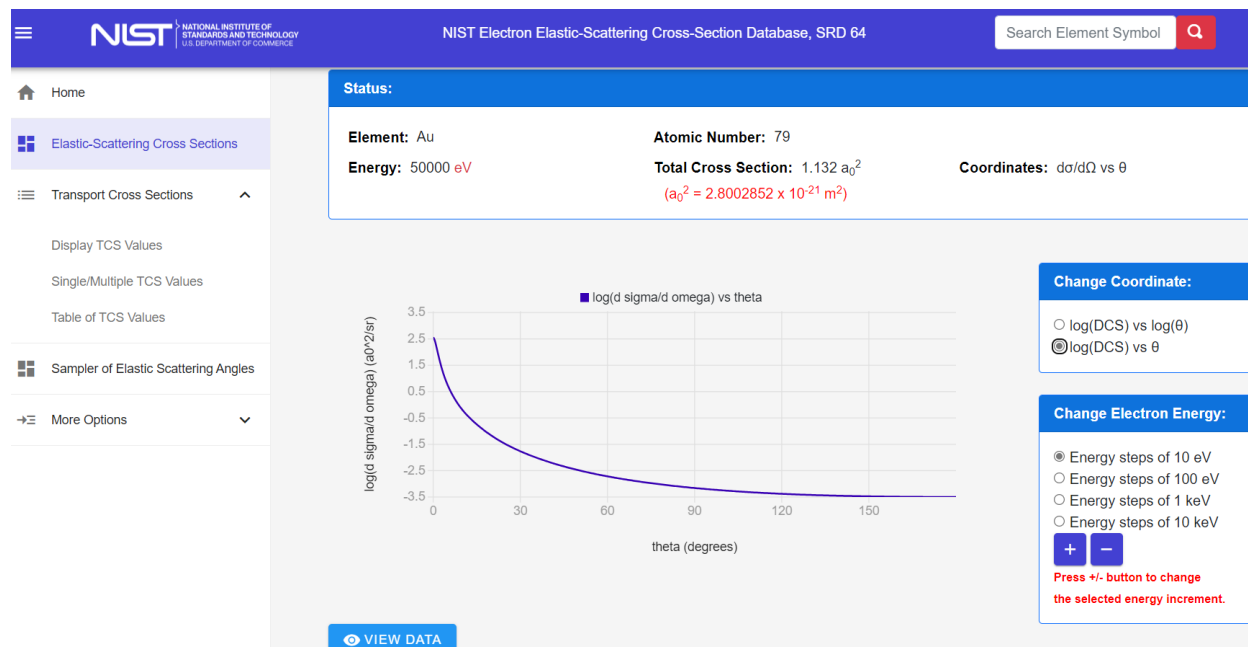


Fig. 5(b). Screen showing the differential cross section for Au in $d\sigma/d\Omega$ versus θ coordinates at 50 keV on semi-logarithmic scales.

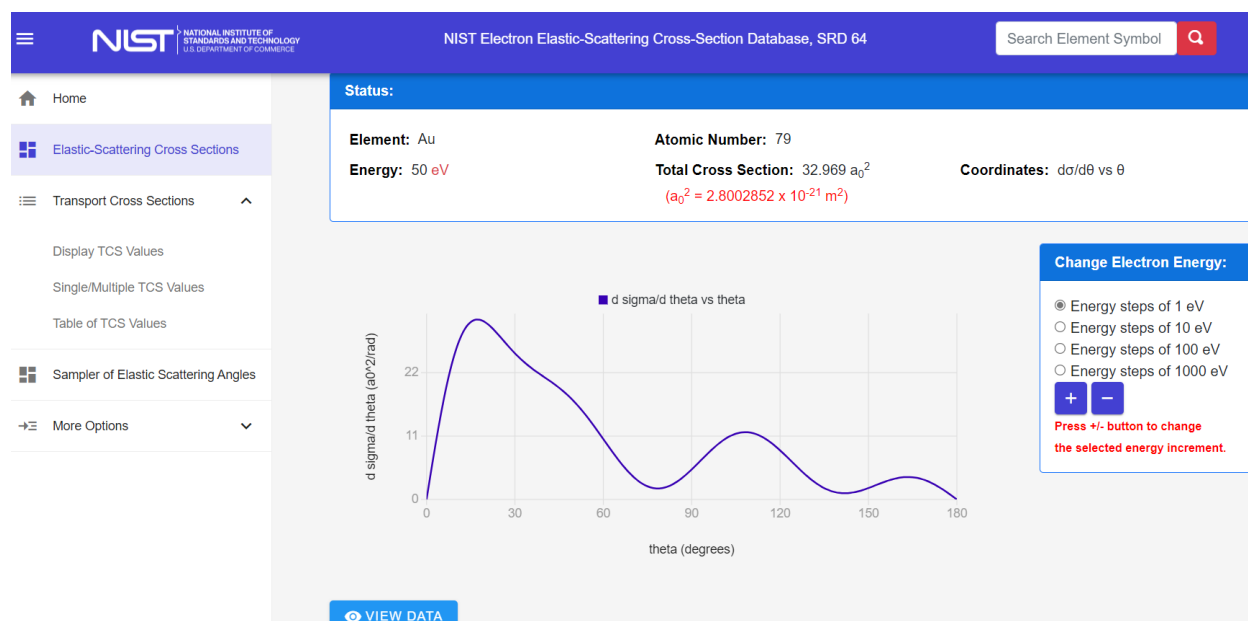


Fig. 6. Screen showing the differential cross section for Au in $d\sigma/d\theta$ versus θ coordinates at 50 eV on linear scales.

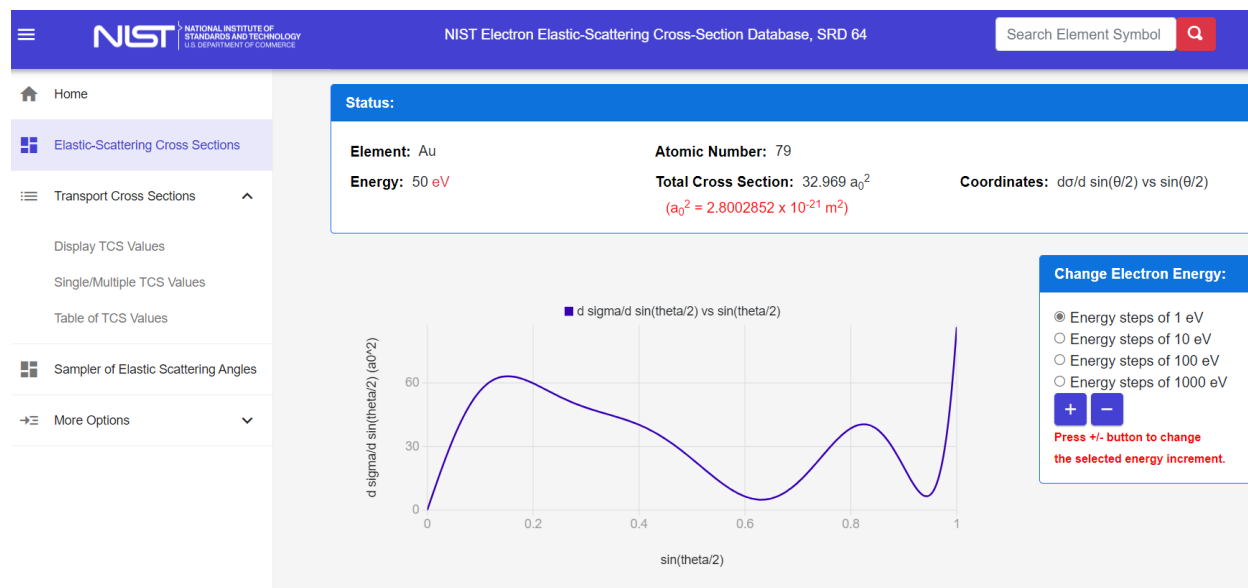


Fig. 7. Screen showing the differential cross section for Au in $d\sigma/d \sin(\theta/2)$ versus $\sin(\theta/2)$ coordinates at 50 eV on linear scales.

Figures 6 and 7 show example plots of the DCS for Au at 50 eV in the $d\sigma/d\theta$ versus θ and $d\sigma/d \sin(\theta/2)$ versus $\sin(\theta/2)$ coordinate systems, respectively.

If the **View Data** button is clicked (e.g., at the bottom of the example screens in Figs. 4 to 7), a Table will appear of the numerical data used in the preparation of the particular plot. The user can

choose to download the data in one of the three available formats (text or CSV files) by clicking on the corresponding **Text Data File** or **CSV Data File** buttons.

2.2 Transport Cross Sections

The definition of the transport cross section is given in Section 3. If the Transport Cross Sections option of the main menu (Fig. 1) is chosen, a submenu of three choices appears:

- (a) Display TCS (transport cross-section) values
- (b) Single/multiple TCS (transport cross-section) values
- (c) Table of TCS (transport cross-section) values

For each option, a screen with the Periodic Table appears (similar to Fig. 2) and the user selects an element of interest. The following screens for options (a), (b), and (c) enable TCS data for the selected element to be displayed graphically as a function of energy, allow TCS data for user-specified energies to be displayed, and enable TCS data to be displayed at regularly spaced electron energies, respectively. Files containing TCS values can be downloaded for all three options. The TCS values are shown in units of a_0^2 .

For option (a), a user will first select an initial energy (between 50 eV and 300 keV), as shown in Fig. 8. In this example, Au had been previously chosen and an initial energy of 1000 eV has been selected.

Fig. 8. Screen for selecting initial electron energy.

TCS values are displayed as a function of electron energy in either of two energy ranges, 50 eV to 20 keV or 1 keV to 300 keV, depending on the user's choice of an initial energy. Example screens are shown in Figs. 9(a) and 9(b) for Au with initial energies of 1000 eV and 50 keV, respectively. A value of the transport cross section for the chosen initial energy is then displayed above the plot. The selected initial energy can be changed by clicking on the **+ energy** or **- energy** buttons; these changes will occur in steps of 1 eV, 10 eV, 100 eV, or 1000 eV depending on the choice of button selected. The energy dependence of the cross section can be displayed on linear, semi-logarithmic, or logarithmic scales; these scales are chosen with the buttons in the upper-right part of the screen.

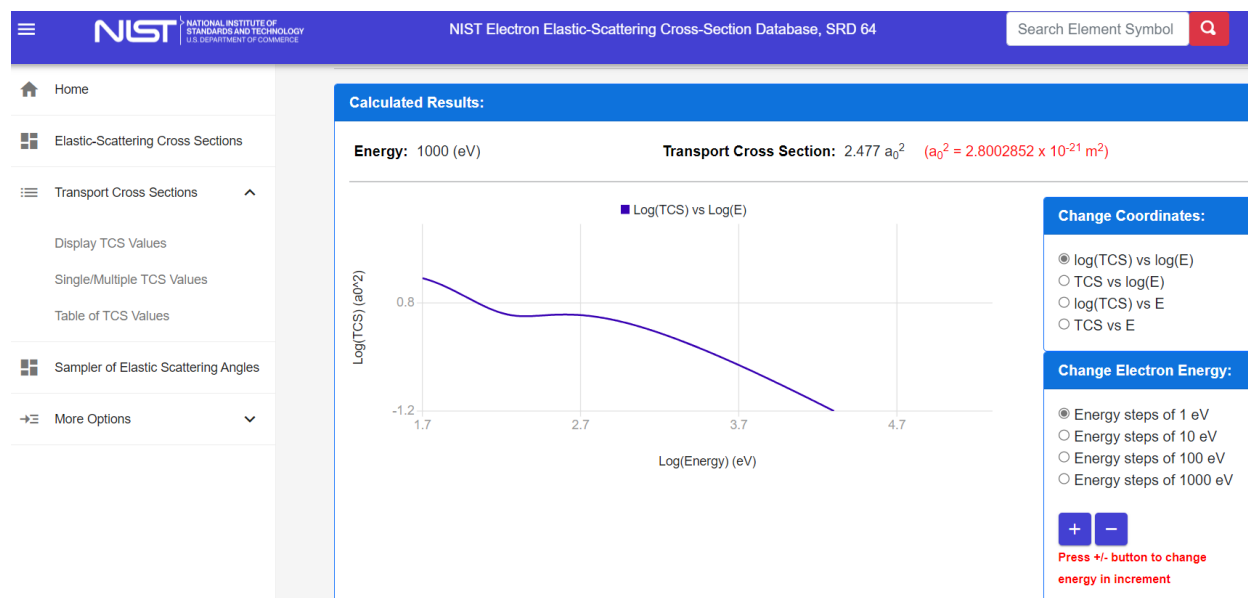


Fig. 9(a). Screen showing the energy dependence of the transport cross section for Au in the energy range from 50 eV to 20 keV.

If the cursor is moved into the area of a graphical display, a box will appear that displays the X,Y values at a selected point.

If the **View Data** button is clicked (e.g., at the bottom of the example screens in Figs. 9(a) and 9(b)), a Table will appear of the numerical data used in the preparation of the particular plot. The user can choose to download the data in one of the two available formats (text or CSV files) by clicking on the corresponding **Text Data File** or **CSV Data File** buttons.

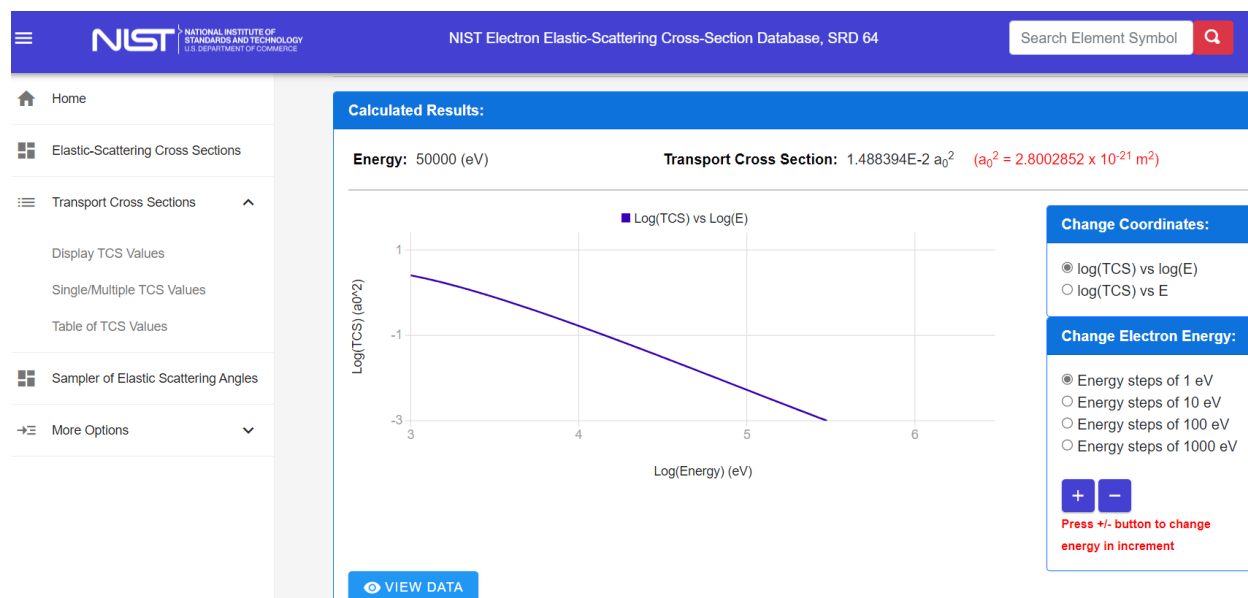


Fig. 9(b). Screen showing the energy dependence of the transport cross section for Au in the energy range from 1 keV to 300 keV.

For option (b), the user can display transport cross sections for one or more electron energies and create files with these values using the screen shown in Fig. 10 (after selection of Au for this example). The user enters the energy value of interest (between 50 eV and 300 keV) in a box. On clicking the **Add** button, the transport cross section for this energy is calculated and displayed in the box in the central part of the screen. Additional energies can be entered in the same way and the corresponding transport cross sections will be displayed in the central box. The user can then choose to download the TCS data in one of the two available file formats.

With option (c), the user can display a Table of transport cross sections at regularly spaced electron energies. The screen of Fig. 11 appears (after selection of Au for this example) and the user enters the number of transport-cross-section values desired (with a maximum of 401 values) and the minimum and maximum energies. The user also chooses whether the electron energies should be distributed linearly or logarithmically in the specified energy range by selecting one of the buttons. After clicking the **Create** button, the Table of cross section values is calculated and displayed as shown in Fig. 12. As for options (a) and (b), a user can choose to download the data in one of the two available formats (text or CSV files) by clicking on the corresponding **Text Data File** or **CSV Data File** buttons.

NIST NATIONAL INSTITUTE OF STANDARDS AND TECHNOLOGY U.S. DEPARTMENT OF COMMERCE

NIST Electron Elastic-Scattering Cross-Section Database, SRD 64

Search Element Symbol

Home

Elastic-Scattering Cross Sections

Transport Cross Sections

Display TCS Values

Single/Multiple TCS Values

Table of TCS Values

Sampler of Elastic Scattering Angles

More Options

Single/Multiple Transport Cross Section Values:

Instructions: Enter an energy and press the Add button to add an energy in its calculated Transport Cross Section (TCS)

Element: Au Atomic Number: 79

Energy: 10000

ADD

Remarks:

- Electron energy should range from 50 eV to 300 keV
- $a_0^2 = 2.8002852 \times 10^{-21} \text{ m}^2$

Single/Multiple Transport Cross Section Values:

[Text Data File](#) [CSV Data File](#)

No.	Energy (eV)	TCS (a_0^2)	Action
1	50	17.016	
2	100	7.008	
3	1000	2.477	
4	10000	1.624083E-1	

Help:

- Press the Add button to add an energy and its calculated Transport Cross Section (TCS) in the following table.
- Press the Delete button to remove a selected row of data

Fig. 10. Transport cross sections calculated for Au at selected energies.

NIST NATIONAL INSTITUTE OF STANDARDS AND TECHNOLOGY U.S. DEPARTMENT OF COMMERCE

NIST Electron Elastic-Scattering Cross-Section Database, SRD 64

Search Element Symbol

Home

Elastic-Scattering Cross Sections

Transport Cross Sections

Display TCS Values

Single/Multiple TCS Values

Table of TCS Values

Sampler of Elastic Scattering Angles

More Options

Table of Transport Cross Section Values:

» Transport Cross Sections » [Table of TCS Values](#)

Create Table of Transport Cross Section Values:

Element: Au Atomic Number: 79

Distribution of TCS Values ☒ Linear Distribution; ☐ Logarithmic Distribution

Number of TCS Values (Max. 401): 401

Minimum Energy (eV): 50 Maximum Energy (eV): 300000

+ CREATE

Remark:

- $a_0^2 = 2.8002852 \times 10^{-21} \text{ m}^2$

Fig. 11. Screen for creating a Table of transport cross section values.

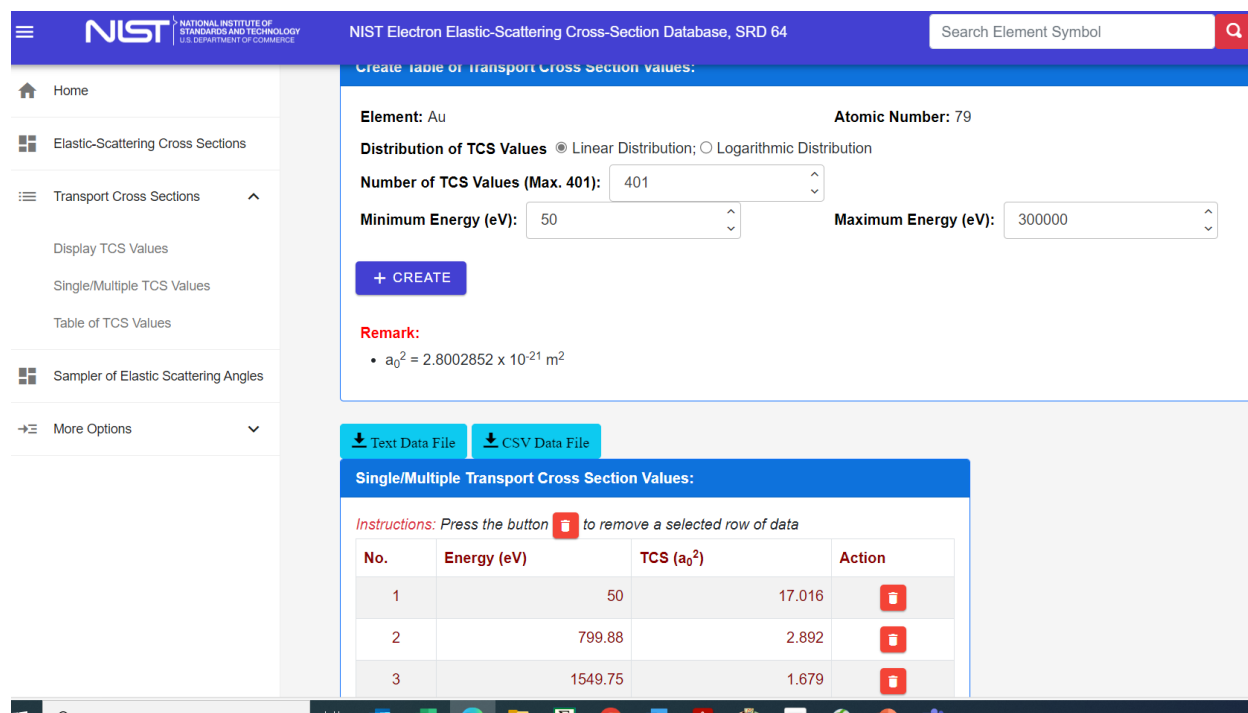


Fig. 12. Screen showing part of a Table of transport cross sections for Au at the indicated energies.

2.3 Sampler of Elastic Scattering Angles

As in Version 3.2 of SRD 64 and earlier versions, the current version provides the Fortran code of the sampler of elastic-scattering angles and the numerical data needed for its use. After clicking on **Sampler of Elastic Scattering Angles**, a Periodic Table of the elements will appear, as shown in Fig. 2. Both the Fortran code and the numerical data for the selected element (in this case calcium) can be downloaded from the screen shown in Fig. 13.

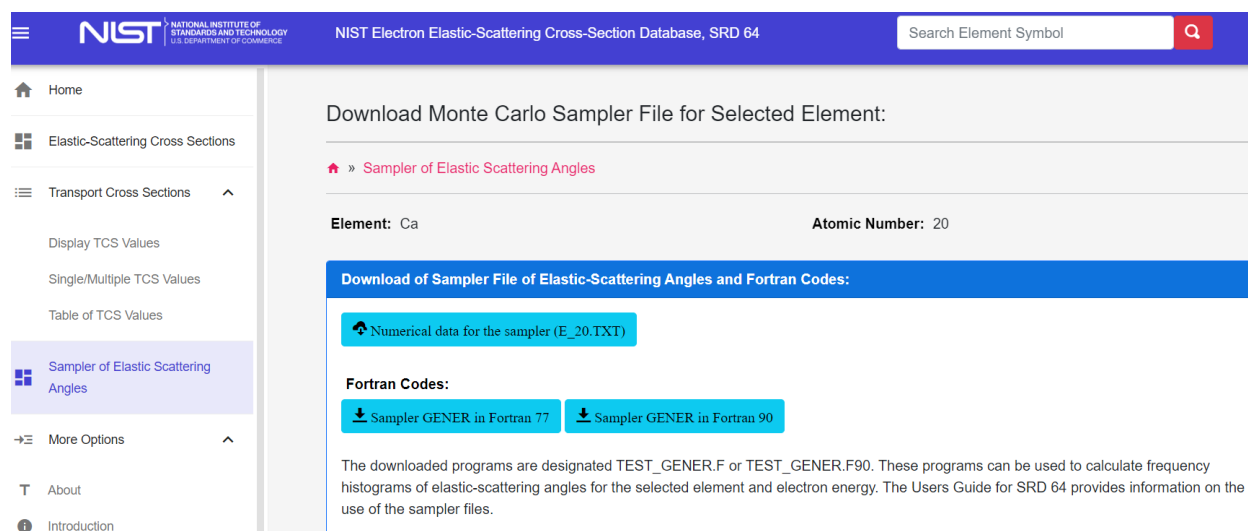


Fig. 13. Screen with options for selecting files for the sampler. This exemplary screen refers to the previously selected element with atomic number $Z = 20$ (calcium).

2.4 Search

The Search box at the top of the Home page (Fig. 1) enables a user to find all data for a selected element. Figure 14 shows the data sets available if the element symbol for gold (Au) was entered in the Search box.

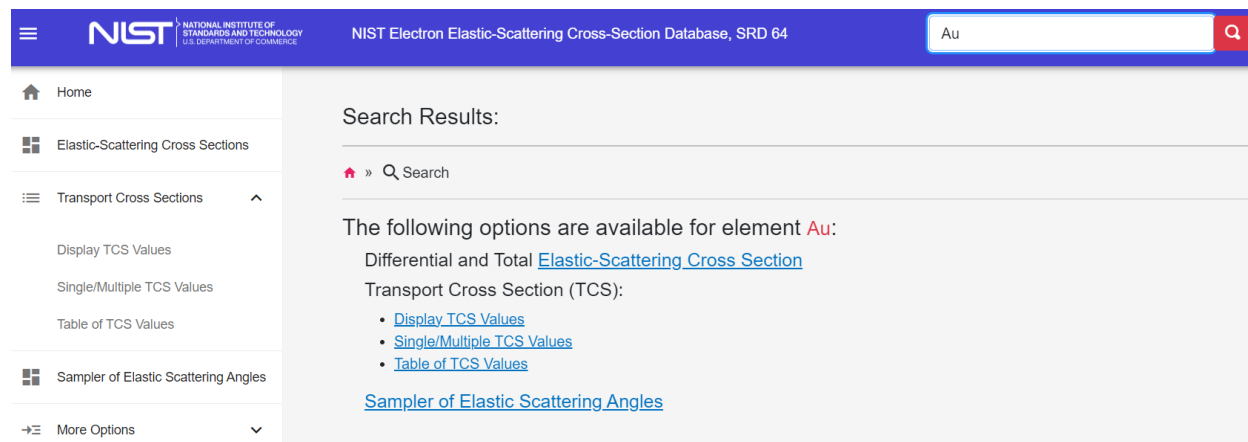


Fig. 14. Screen showing the results of a search for available data for gold (Au).

2.5 More Options

The **More Options** button on the introductory screen (Fig. 1) allows the user to access the following information:

- **About** (with basic information on the database and two references [1,2] that discuss evaluation of the data, methods of determination, and uncertainty)
- **Introduction** (with the text given on the introductory screen)
- **Acknowledgments**
- **Version History**
- **Disclaimers**
- **Citation Guide**
- **Contact Information**

3. Theory

3.1 Differential Cross Sections for Elastic Scattering

The differential cross sections (DCSs) for elastic scattering were calculated using the relativistic Dirac partial-wave analysis, as described by Walker [3]. The scattering potential was obtained from the self-consistent Dirac-Hartree-Fock (DHF) density for free atoms [4] with the local exchange potential of Furness and McCarthy [5]. The numerical calculations were performed with the algorithm described by Salvat and Mayol [6]. Further details are given elsewhere [1,2].

The DCS is related to the phase shifts, δ_l^\pm , of order l by the following expressions [3]:

$$d\sigma_e / d\Omega = |f(\theta)|^2 + |g(\theta)|^2, \quad (1)$$

where $f(\theta)$ and $g(\theta)$ are the direct and indirect scattering amplitudes, respectively, given by:

$$f(\theta) = \frac{1}{2iK} \sum_l \left\{ (l+1)[\exp(2i\delta_l^+) - 1] + l[\exp(2i\delta_l^-) - 1] \right\} P_l(\cos\theta) \quad (2)$$

$$g(\theta) = \frac{1}{2iK} \sum_l [\exp(2i\delta_l^-) - \exp(2i\delta_l^+)] P_l^1(\cos\theta). \quad (3)$$

In Eqs. (2) and (3), $P_l(\theta)$ are Legendre polynomials, and $P_l^1(\theta)$ are associated Legendre polynomials:

$$P_l^1(z) = (1-z^2)^{1/2} \frac{dP_l(z)}{dz}.$$

The phase shifts δ_l^\pm are obtained from the large- r behavior of the radial wave functions, $P_l^\pm(r)$ and $Q_l^\pm(r)$ which are calculated by integrating the radial Dirac equations:

$$\frac{dP_l^\pm}{dr} = -\frac{k^\pm}{r} P_l^\pm(r) + \frac{E-V+2mc^2}{c\hbar} Q_l^\pm(r) \quad (4a)$$

$$\frac{dQ_l^\pm}{dr} = -\frac{E-V}{c\hbar} P_l^\pm(r) + \frac{k^\pm}{r} Q_l^\pm(r), \quad (4b)$$

where E is the kinetic energy of the projectile electron that is related to its total energy W by $E = W - mc^2$, $V(r)$ is the interaction potential as a function of radius r , m is the electron rest mass, and c is the velocity of light. The solution algorithm implements Bühring's power-series method [7] and is based on a cubic-spline interpolation of the potential function $rV(r)$ which is tabulated on a dense grid of r values,

$$r_1 = 0 < r_2 \cdots < r_{N-1} < r_N. \quad (5)$$

That is, between each pair of consecutive grid points, r_n and r_{n+1} , the potential function, $rV(r)$, is represented as a piecewise cubic polynomial in r :

$$rV(r) = a_n + b_n r + c_n r^2 + d_n r^3. \quad (6)$$

Then, in the interval (r_n, r_{n+1}) , the radial functions can be formally expressed by power series:

$$P_l^\pm(r) = r^\alpha \sum_{i=0}^{\infty} p_i r^i \quad Q_l^\pm(r) = r^\beta \sum_{i=0}^{\infty} q_i r^i, \quad (7)$$

with coefficients determined by the values of $P_l^\pm(r_n)$ and $Q_l^\pm(r_n)$ at the end point of the interval. As these series expansions can be summed up to the required accuracy (9 significant digits in the code), truncation errors are practically avoided.

The interaction potential $V(r)$ is defined as:

$$V(r) = -e\varphi(r) + V_{exc}(r), \quad (8)$$

where $\varphi(r)$ is the electrostatic potential of the target atom:

$$\varphi(r) = \frac{Ze}{r} - e \left(\frac{1}{r} \int_0^r \rho(r') 4\pi r'^2 dr' + \int_r^\infty \rho(r') 4\pi r' dr' \right), \quad (9)$$

and where $\rho(r)$ is the atomic electron density that was calculated using the self-consistent DHF code of Desclaux [4].

The term $V_{exc}(r)$ in Eq. (8) is a local approximation to the exchange interaction between the projectile and the electron in the target; it should not be confused with the exchange interaction considered in self-consistent calculations that accounts for exchange between atomic electrons. We use the exchange potential of Furness and McCarthy [5]:

$$V_{exc}(r) = \frac{1}{2} [E + e\varphi(r)] - \frac{1}{2} \left\{ [E + e\varphi(r)]^2 + 4\pi \frac{\hbar^2 e^2}{m} \rho(r) \right\}^2. \quad (10)$$

The interaction potential [Eq. (8)] is thus completely determined by the atomic density $\rho(r)$.

The integration of the radial equations is started from $r = 0$, with boundary values:

$$P_l^\pm(0) = 0, \quad Q_l^\pm(0) = 0. \quad (11)$$

In the first r -interval from $r_1 = 0$ to r_2 [Eq. (5)], the constants α and β [Eq. (7)] are different from zero and determined by the angular momentum quantum numbers [8]. For the outer intervals ($r > r_2$), $\alpha = \beta = 0$.

After determining the values of the radial functions at r_2 , the solution is extended outwards by using the series expansions [Eq. (7)] (with $\alpha = \beta = 0$) up to a certain radial distance r_{\max} , large

enough to ensure that the potential energy of the electron $V(r)$ is negligible as compared to its kinetic energy E . For selected elements and at an energy of 10 keV, the maximum ranges, r_{\max} , were as follows (in a_0 units):

for $Z = 1$	$r_{\max} = 12.27$
for $Z = 13$	$r_{\max} = 20.15$
for $Z = 28$	$r_{\max} = 17.85$
for $Z = 47$	$r_{\max} = 19.37$
for $Z = 79$	$r_{\max} = 17.11$
for $Z = 96$	$r_{\max} = 21.54$

At an energy of 20 000 eV:

for $Z = 1$	$r_{\max} = 11.96$
for $Z = 13$	$r_{\max} = 19.75$
for $Z = 28$	$r_{\max} = 17.48$
for $Z = 47$	$r_{\max} = 18.80$
for $Z = 79$	$r_{\max} = 16.74$
for $Z = 96$	$r_{\max} = 21.13$

At sufficiently large distances r , the radial function $P_l^\pm(r)$ adopts the asymptotic form:

$$P_l^\pm(r) \cong \sin(Kr - l \frac{\pi}{2} + \delta_l^\pm), \quad (12)$$

where

$$\hbar K = \frac{1}{c} \sqrt{E(E + 2mc^2)} \quad (13)$$

is the momentum of the projectile. Equation (12), which confers a geometrical meaning to the phase shift, is not directly usable to compute δ_l^\pm because $P_l^\pm(r)$ reaches the form given by Eq. (12) only at distances r that may be much larger than r_{\max} . Instead, the phase shift is obtained from the calculated values of the radial functions at r_{\max} by matching the numerical solution to the exact solution for $r > r_{\max}$ ($V = 0$) which can be expressed as a linear combination of spherical Bessel functions, $j_k(Kr)$ and $n_k(Kr)$ of indices $k = l, l \pm 1$ [8].

A considerable number of phase shifts was found to be necessary to achieve 8-digit accuracy in the calculation of DCSs from Eqs. (1) to (3). At an energy of 10 000 eV, we have:

$$\text{for } Z = 1 \quad 0 \leq l \leq 221$$

for Z = 13	$0 \leq l \leq 386$
for Z = 28	$0 \leq l \leq 343$
for Z = 47	$0 \leq l \leq 369$
for Z = 79	$0 \leq l \leq 325$
for Z = 96	$0 \leq l \leq 422$

At an energy of 20 000 eV:

for Z = 1	$0 \leq l \leq 307$
for Z = 13	$0 \leq l \leq 538$
for Z = 28	$0 \leq l \leq 478$
for Z = 47	$0 \leq l \leq 514$
for Z = 79	$0 \leq l \leq 452$
for Z = 96	$0 \leq l \leq 589$

The only special functions used in calculations of the DCSs for the DHF potential are spherical Bessel functions $j_l(x)$ and $n_l(x)$. The algorithm used to compute these functions combines several analytical expressions and recurrence relations, and yields results that are accurate to 13 or more significant digits. The code used for these calculations was tested for $0 \leq l \leq 20\,000$ and $0 < x < 20\,000$.

3.2 Transport Cross Sections

Transport cross sections are needed for determination of numerous parameters related to electron transport in solids (the depth distribution function, the effective attenuation length, the electron mean escape depth, etc.) [9, 10]. The transport cross section describes the mean fractional momentum loss due to elastic scattering alone. We denote by \mathbf{k} the electron momentum before elastic scattering, and by \mathbf{k}' , the projection of the momentum after elastic scattering on the initial direction. Obviously, $\mathbf{k}' = \mathbf{k} \cos \theta$. We further denote the fractional momentum loss, due to elastic scattering alone, by

$$\Delta k = \frac{|\mathbf{k} - \mathbf{k}'|}{|\mathbf{k}|}.$$

The transport cross section is the product of the mean fractional momentum loss and the total elastic-scattering cross section:

$$\sigma_{tr} = \sigma_{el} \langle \Delta k \rangle = \sigma_{el} \frac{\int \Delta k (d\sigma / d\Omega) d\Omega}{\int_{4\pi} (d\sigma / d\Omega) d\Omega}. \quad (14)$$

Equation (14) can be transformed to:

$$\sigma_{tr} = 2\pi \int_0^{\pi} (1 - \cos \theta) (d\sigma / d\Omega) \sin \theta d\theta. \quad (15)$$

A change of the atomic potential leads to pronounced variation of the differential elastic-scattering cross section for small scattering angles and rather small variations for larger scattering angles [10]. In the integrand of Eq. (15), we have two functions approaching zero for small scattering angles: $\sin \theta$ and $(1 - \cos \theta)$. Consequently, we may expect that the sensitivity of the transport cross section to the interaction potential is much smaller than the sensitivity of the total elastic-scattering cross section. It has been shown that the transport cross sections values depend very weakly on the potential for elements with a wide range of atomic numbers (Be to Au) and for electron energies from 100 eV to 10 000 eV [11].

4. References

- [1] A. Jablonski, F. Salvat, and C. J. Powell, J. Phys. Chem. Ref. Data **33**, 409 (2004).
- [2] F. Salvat, A. Jablonski, and C. J. Powell, Computer Physics Communications **165**, 1571 (2005).
- [3] D. W. Walker, Advances in Physics **20**, 257 (1971).
- [4] J. P. Desclaux, Computer Physics Communications **9**, 31 (1975); erratum ibid **13**, 71 (1977).
- [5] J. B. Furness and I. E. McCarthy, J. Phys. B: At. Mol. Phys. **6**, 2280 (1973).
- [6] F. Salvat and R. Mayol, Computer Physics Communications **74**, 358 (1993).
- [7] W. Bühring, Z. Phys. **187**, 180 (1965).
- [8] F. Salvat and R. Mayol, Comput. Phys. Comm. **62**, 65 (1991).
- [9] A. Jablonski and C. J. Powell, J. Electron Spectrosc. Relat. Phenom. **100**, 137 (1999).
- [10] A. Jablonski and C. J. Powell, Surf. Science Reports **47**, 33 (2002).
- [11] A. Jablonski and C. J. Powell, Surf. Science **463**, 29 (2000).

APPENDIX A

SAMPLER OF ELASTIC SCATTERING ANGLES

As in Version 3.2 of SRD 64 and earlier versions, the current version provides the Fortran code of the sampler of elastic-scattering angles and the numerical data needed for its use. Both the Fortran code and the numerical data can be downloaded from the screen shown in Fig. A1.

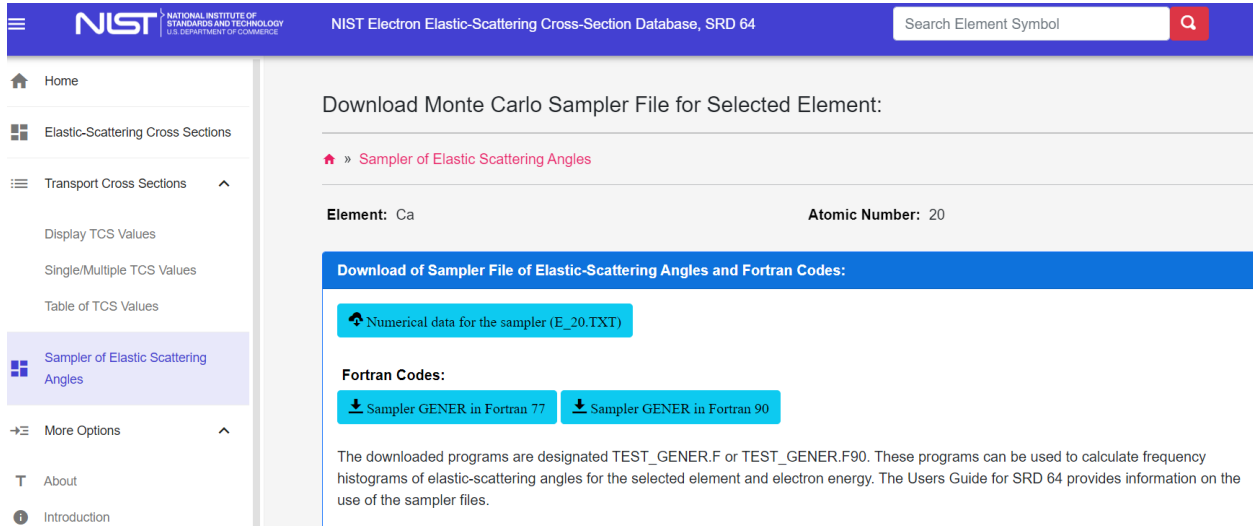


Fig. A1. Screen with options for selecting files for the sampler. This exemplary screen refers to the previously selected element with atomic number $Z = 20$ (calcium).

The code of the sampler GENER is the implementation of the transformation method [1,2] based on the inverse cumulative probability density distribution. The downloaded program TEST_GENER provides the histograms of the generated scattering angles. The sampler code was tested using the Fortran 77 compiler and the Fortran 90 compiler. In both cases, the same results were obtained. The interested user could include the code GENER from the downloaded program into a Monte Carlo program for describing electron transport in matter. The only requirement for calculations of this type is the presence of the file E_&&.TXT where the characters && indicate a given atomic number. This file contains the needed input data and must be located in the same directory as the Monte Carlo program.

The numerical method

The cumulative probability density (CPD) distribution function, $\Phi(\Theta)$, is defined as the probability that the generated polar angle θ for elastic scattering does not exceed a certain angle Θ . We have:

$$\Phi(\Theta) = \frac{2\pi}{\sigma_{tot}} \int_0^{\Theta} \frac{d\sigma}{d\Omega} \sin \theta d\theta \quad (A1)$$

where $d\sigma/d\Omega$ is the differential cross section for elastic scattering and σ_{tot} is the total cross section for elastic scattering. On introducing the new variable $x = \cos \theta$ into the integral in Eq. (A1), we obtain:

$$\Phi(X) = \int_x^1 f(x) dx \quad (\text{A2})$$

where $X = \cos \theta$ and $f(x)$ is the probability density function of cosines of the elastic-scattering angle.

$$f(x) = \frac{1}{\sigma_{tot}} \frac{d\sigma}{dx} \quad (\text{A3})$$

Examples of CPD functions calculated from Eq. (A2) are shown in Fig. A2. Let us assume that the X values are realizations of the random variable with probability density distribution $f(x)$. On transformation of this random variable using Eq. (A2), we obtain the random variable $\Phi(X)$. It can be proved that this random variable is described by a uniform probability density distribution. This result is the basis for the method of generating the distribution of elastic-scattering angles, θ . Let us denote by R the value generated from a random number generator in the range from zero to unity. We have

$$R = \Phi(X) \quad (\text{A4})$$

or

$$\Phi^{-1}(R) = X = \cos \theta \quad (\text{A5})$$

where $\Phi^{-1}(R)$ is the inverse CPD function.

The file E_&&.TXT with numerical data for the sampler GENER contains the set of CPD functions calculated for 101 energies distributed logarithmically in the range from 50 eV to 20 keV, *i.e.*, the set of functions visualized in Fig. A2 for copper and gold. To calculate a given angle θ , we need to solve Eq. (A5). This procedure is illustrated in Fig. (A3) for copper at 150 eV. As shown in this figure, for the random value $R = 0.547$ we obtain the scattering angle of $\theta = 41.2^\circ$.

Example of calculations

Let us run the downloaded program TEST_GENER for the case shown in Fig. A3. On starting the program, the user is prompted to provide the atomic number, energy in eV, number of generated angles, and the number of intervals in the histogram. On completing the run, the file with results is created with general designation HIST_&&\$.TXT where the string \$\$\$\$ designates the electron energy in eV. For the considered case, we should obtain the file HIST_2900150.TXT. A fragment of the content of this file is shown in Fig. A4:

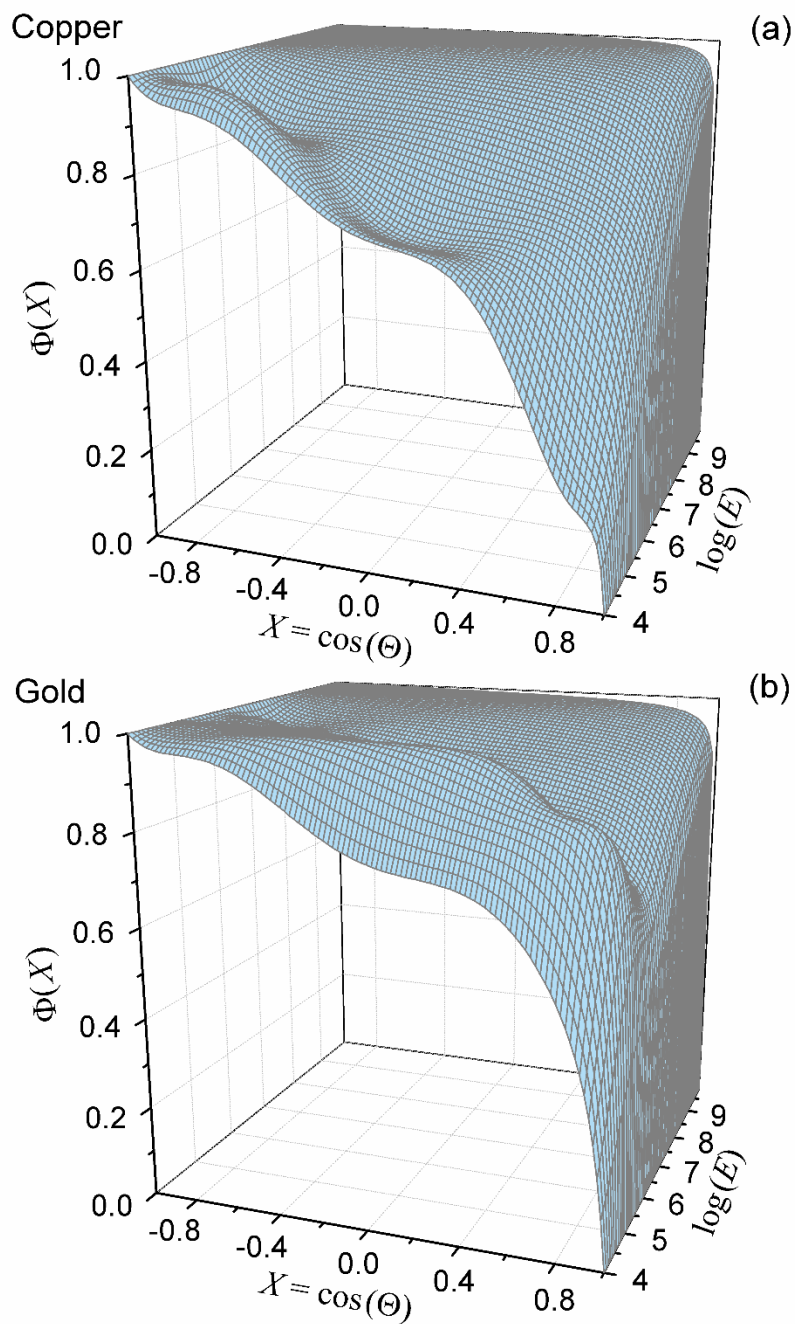


Fig. A2. The CPD functions, $\Phi(X)$, calculated for copper and gold in the energy range from 50 eV to 20 keV.

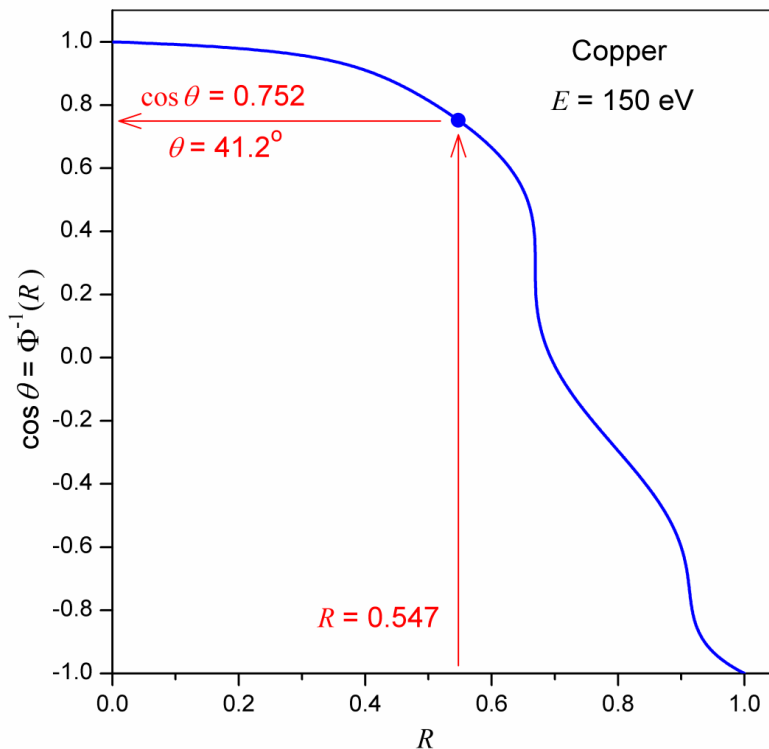


Fig. A3. Plot of the inverse CPD function for copper at 150 eV.

Atomic number	:	29	
Electron energy	:	150.0 eV	
Total cross-section	:	10.596	a0**2
Number of generated angles	:	1000000	
Number of intervals	:	90	

theta (deg)	d sigma/d omega (a0**2/sterad)	d sigma/d theta (a0**2/rad)
1.00	23.494	2.5763
3.00	22.480	7.3922
5.00	20.249	11.089
7.00	17.234	13.196
9.00	14.320	14.075
11.00	11.350	13.608
... (78 lines removed) ...		
169.00	1.3835	1.6586
171.00	1.4234	1.3991
173.00	1.5068	1.1538
175.00	1.6186	0.88639
177.00	1.6367	0.53821
179.00	1.6720	0.18335

Fig. A4. The file HIST_29_00150.TXT.

As shown in the above listing, the frequency histogram was created after generating 10^6 scattering angles with 90 intervals. The frequency histogram was created in a form that enables

direct comparison with the differential elastic-scattering cross sections (DCS), $d\sigma/d\Omega$ or $d\sigma/d\theta$, in units $a_0^2/sterad$ or a_0^2/rad , respectively. The angular width of the interval in the histogram is equal to 2° in this example. Note that values of the scattering angles, θ , listed in Fig. A4 refer to the centers of consecutive intervals. This choice facilitates comparison with the corresponding cross sections.

It is important to note that the numerical method for the sampler in Version 3.2 of SRD 64 (and in earlier versions) is different from the sampler presently implemented. Previously, the basis for the sampler was the so-called composite method [3,4]. Unfortunately, this sampler is less accurate in cases when the differential elastic-scattering cross section values vary over a wide range. A particularly acute case is the DCS for hydrogen at the highest energy considered, *i.e.*, at 20 keV, where the DCS, $d\sigma/d\Omega$, varies over seven orders of magnitude.

A comparison of histograms obtained from the two samplers in the $d\sigma/d\theta$ versus θ coordinate system is shown in Fig. A5. We see that the old sampler fails to estimate correctly the probability for generating elastic-scattering angles greater than about 30° . The histogram obtained from the new sampler practically reproduces the DCS over the full angular range.

We also point out that the old sampler (also with the name GENER) required the presence of a file designated E&&.D64 with the numerical data for a selected element with atomic number &&. The content of this file is different from the content of the file E_&&.TXT that can be downloaded from Version 5 of SRD 64. We recommend that the E&&.D64 files not be used.

- [1] W. H. Press, S. A. Teukolsky, W. T. Vetterling, and B. P. Flannery, *Numerical recipes. The art of scientific computing*, 3rd Edition, Cambridge University Press, Cambridge (2007), pp 362-363.
- [2] A. Jablonski, Series representation of differential elastic scattering cross section for electrons: Application in theoretical models of electron transport in condensed matter, *Comp. Phys. Comm.* (to be published).
- [3] A. Jablonski and S. Tougaard, Database of relativistic elastic scattering cross-sections for calculations of photoelectron and Auger electron transport, *Surf. Interface Anal.* 22 (1994) 129-133.
- [4] J. M. Hammersley and D. C. Hanscomb, *Monte Carlo Methods*, Methuen, London (1967), pp. 36-40.

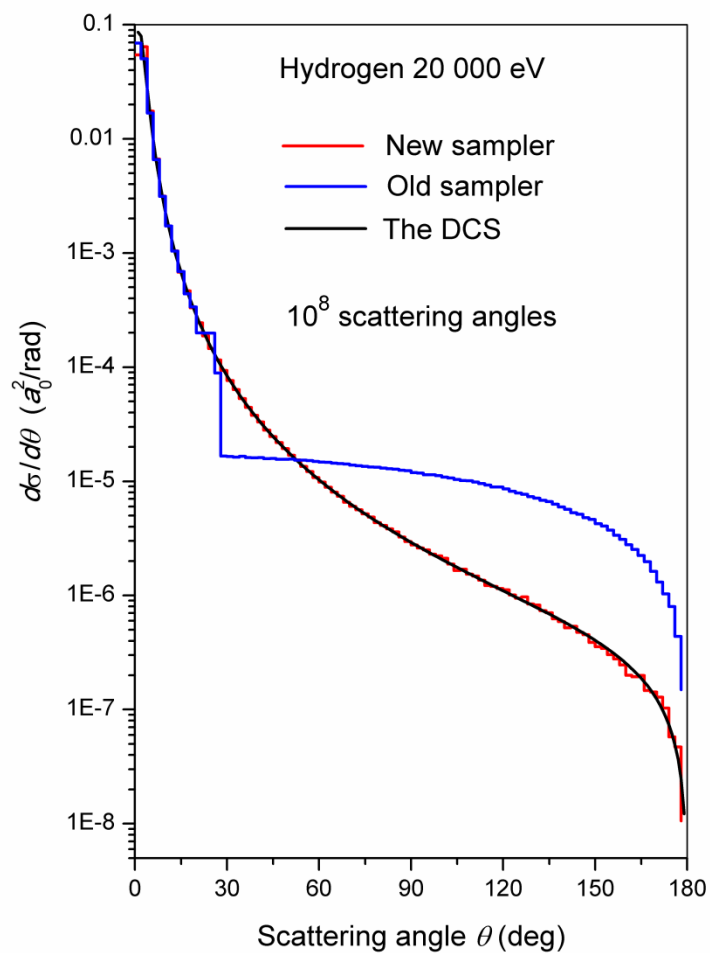


Fig. A5. Comparison of histograms obtained from the old and new samplers with the DCS for hydrogen at 20 keV (in coordinates $d\sigma/d\theta$ versus θ).

APPENDIX B CONTACTS

If you have comments or questions about the database, the Standard Reference Data Program would like to hear from you. Also, if you have any problems with the database, please let us know by contacting:

National Institute of Standards and Technology
Standard Reference Data Program
100 Bureau Drive, Stop 2310
Gaithersburg, MD 20899-2310
Internet: srdata@nist.gov

If you have technical questions relating to the data, contact:

Prof. F. Salvat
Facultat de Física (ECM)
Universitat de Barcelona
Diagonal 647
08028 Barcelona, Spain
Email: cesc@ecm.ub.es

Prof. Dr. A. Jablonski
Institute of Physical Chemistry
Polish Academy of Sciences
Ul. Kasprzaka 44/52
01-224 Warsaw, Poland
Email: ajablonski@ichf.edu.pl

Dr. C. J. Powell
National Institute of Standards and Technology
Materials Measurement Science Division
100 Bureau Drive, Stop 8370
Gaithersburg, MD 20899-8370
Email: cedric.powell@nist.gov